

Optimizing Sparse Generalized Singular Vectors for Feature Selection in Proximal Support Vector Machines with Application to Breast and Ovarian Cancer Detection

Ugochukwu O. Ugwu*¹ and Michael Kirby²

¹Department of Electrical and Computer Engineering, Tufts University, Medford, MA 02155, USA

²Department of Mathematics, Colorado State University, CO 80523, USA

Abstract

This paper presents approaches to compute sparse solutions of Generalized Singular Value Problem (GSVP). The GSVP is regularized by ℓ_1 -norm and ℓ_q -penalty for $0 < q < 1$, resulting in the ℓ_1 -GSVP and ℓ_q -GSVP formulations. The solutions of these problems are determined by applying the proximal gradient descent algorithm with a fixed step size. The inherent sparsity levels within the computed solutions are exploited for feature selection, and subsequently, binary classification with non-parallel Support Vector Machines (SVM). For our feature selection task, SVM is integrated into the ℓ_1 -GSVP and ℓ_q -GSVP frameworks to derive the ℓ_1 -GSVPSVM and ℓ_q -GSVPSVM variants. Machine learning applications to cancer detection are considered. We remarkably report near-to-perfect balanced accuracy across breast and ovarian cancer datasets using a few selected features.

Key words: binary classification, data integration, feature selection, machine learning, optimization, sparse generalized singular vectors, support vector machine, regularization

1 Introduction

We are concerned with the iterative solutions of large-scale minimization problem

$$\min_{\mathbf{z}_i \in \mathbb{R}^m} \frac{\|A_i \mathbf{z}_i\|_2^2}{\|A_j \mathbf{z}_i\|_2^2}, \quad i, j \in \{1, 2\}, \quad i \neq j, \quad (1.1)$$

where $A_1 \in \mathbb{R}^{\ell \times m}$, and $A_2 \in \mathbb{R}^{p \times m}$. We will refer to (1.1) as the Generalized Singular Value Problem (GSVP). Problems of this kind were first considered in [7], and referred to as the variational formulation of the Generalized Singular Value Decomposition [11, GSVD]. Here, we are interested in the extrema of the objective function in (1.1).

In contrast to [7], our goal in this paper is to determine sparse solutions of (1.1) for $\ell \geq p \gg m$ and $m \gg \ell \geq p$. In both situations, \mathbf{z}_i , $i = 1, 2$, are approximations of the generalized singular vectors corresponding to the smallest and largest generalized singular values of the GSVD of A_i and A_j . We will exploit inherent sparsity levels in the computed solutions to carry out feature (gene) selection, and subsequently, perform binary class classification using non-parallel or proximal support vector machines [19].

We begin with the overdetermined case, where $\ell \geq p \gg m$. Without loss of generality, let $i = 1$ and $j = 2$. Then the GSVD [11] of A_1 and A_2 is defined by

$$\begin{aligned} U_1^T A_1 X &= \text{diag}[\alpha_1, \alpha_2, \dots, \alpha_m], \\ U_2^T A_2 X &= \text{diag}[\beta_1, \beta_2, \dots, \beta_m], \end{aligned} \quad (1.2)$$

where $U_1 \in \mathbb{R}^{\ell \times \ell}$ and $U_2 \in \mathbb{R}^{p \times p}$ are orthogonal matrices, and their columns correspond to the left generalized singular vectors of A_1 and A_2 , respectively. Throughout this paper, the superscript T denotes transposition.

The square matrix, $X = [\mathbf{x}_1, \mathbf{x}_2, \dots, \mathbf{x}_m] \in \mathbb{R}^{m \times m}$, is nonsingular, and is shared by A_1 and A_2 . The column vectors, \mathbf{x}_k , $k = 1, 2, \dots, m$, are referred to as the right generalized singular vectors of A_1 and A_2 . They satisfy:

$$\beta_k^2 A_1^T A_1 \mathbf{x}_k = \alpha_k^2 A_2^T A_2 \mathbf{x}_k, \quad k = 1, 2, \dots, m, \quad (1.3)$$

*Corresponding author: Ugochukwu.Ugwu@tufts.edu, uugobinnah@gmail.com

where the ratios $\{\alpha_1/\beta_1, \alpha_2/\beta_2, \dots, \alpha_m/\beta_m\}$ are the generalized singular values of the matrix pair $\{A_1, A_2\}$ such that $\alpha_k^2 + \beta_k^2 = 1$, $k = 1, 2, \dots, m$. The smallest generalized singular values of $\{A_i, A_j\}$ are the stationary values of (1.1), and the corresponding right singular vectors are the stationary vectors [11].

An advantage of the GSVP is that it eliminates the need to form symmetric matrices, $A_1^T A_1$ and $A_2^T A_2$ [11]. This is particularly beneficial for large-scale problems, with more columns than rows ($\ell \geq p \gg m$), as often encountered in biological settings, such as gene expression studies, where computing both matrix-matrix products is quite prohibitive, and moreover, impractical even with enormous computational power. However, when explicit formation of $A_1^T A_1$ and $A_2^T A_2$ can be afforded, and the denominator of (1.1) is positive definite, we may refer to (1.1) as the Generalized Eigenvalue Problem (GEP); see [24]. In this case, the solutions of (1.1) correspond to the generalized eigenvectors associated with the smallest generalized eigenvalues, λ_i of $\{A_i^T A_i, A_j^T A_j\}$, $i, j \in \{1, 2\}, i \neq j$.

The connections between the GSVP and GEP are straightforward to establish [11] for $\ell \geq p \gg m$. This follows, since the generalized eigenvalues of $\{A_1^T A_1, A_2^T A_2\}$ are the square of the generalized singular values of $\{A_1, A_2\}$, i.e., $\lambda_k = \alpha_k^2/\beta_k^2$, $k = 1, 2, \dots, m$. Moreover, the right generalized singular vectors of $\{A_1, A_2\}$ are the generalized eigenvectors of $\{A_1^T A_1, A_2^T A_2\}$.

When $m \gg \ell \geq p$, the minimization problem (1.1) is underdetermined. Therefore, establishing a connection between the GSVP and GEP becomes very challenging. This is due to the non-uniqueness of the solutions of (1.1). Specifically, (1.1) can have infinitely many solutions since $N(A_i) \cap N(A_j) \neq \mathbf{0}$, where $N(M)$ is the null space of the matrix M and $\mathbf{0}$ is the zero vector [14]. This makes determining accurate and stable optimal solutions of (1.1) that are less sensitive to noise and errors in the data matrices infeasible.

To remedy the challenges associated with solving (1.1), we introduce regularization by replacing (1.1) with nearby problems that can be solved stably. This leads to the following regularized problems:

$$\min_{\mathbf{z}_i \in \mathbb{R}^m} \frac{\|A_i \mathbf{z}_i\|_2^2}{\|A_j \mathbf{z}_i\|_2^2} + \delta_i \|\mathbf{z}_i\|_1, \quad i, j \in \{1, 2\}, \quad i \neq j, \quad (1.4)$$

where δ_i is the regularization parameter that influences the accuracy and stability of the solutions of (1.1). It is well known that different values of δ_i have varying impact on the solutions of (1.1), and the optimal parameter choices depend on the data matrices and applications of interest. Here and below, we will refer to the first and second terms in (1.4) as the *fidelity* and *regularization* terms, respectively.

We also will refer to the minimization problems (1.4) as the ℓ_1 -GSVP. The use of ℓ_1 -norm in (1.4) is to promote sparsity in the computed (approximate) generalized singular vectors. As such, only the non-zero elements of \mathbf{z}_i are utilized for feature selection. The sparsity enhancing property of ℓ_1 penalty has been widely adopted in the literature; see, e.g., [31, 5], but the novelty of our contributions lie in its application in the context of (1.4).

It is the purpose of this paper to develop new strategies for computing sparse solutions of (1.1), and then discuss how sparsity in the computed solutions can be exploited to carry out feature selection and binary classification tasks. In our specific applications, such as microarray data analysis, the number of non-zero elements in the solutions of (1.4) directly correspond to the most relevant and informative genes in A_1 and A_2 , while genes associated with “near-zero” coefficients are considered irrelevant or redundant. When the solutions of (1.4) are very sparse, only a small number of features will be selected. This drastically reduces the dimensionality of the data matrices, resulting in improved robustness to noise, as well as the accuracy and efficiency of subsequent analyses, such as breast and ovarian cancer classification.

The GSVD (without ℓ_1 penalty) has been extensively employed for gene selection purposes in the literature; see, e.g., [1, 3]. In particular, a *gene shaving* [16] approach described in [3] focuses on selecting the most variant genes across several cancer cell lines and tumor samples. This method iteratively projects each gene onto a chosen projection direction determined by the generalized singular values. Then progressively shaves off the least variant group of genes with the smallest positive and negative projection scores. It is noteworthy that the utilization of the GSVD projections in a non-iterative manner, for gene selection and simultaneous low-rank reconstruction of gene expression datasets, was first proposed in [1]. An extension of this idea to higher-order GSVD for gene selection is presented in, e.g., [26, 22].

We are also interested in computing approximate solutions of (1.1) with a greater degree of sparsity than in (1.4). This is motivated by our desire to determine a parsimonious set of predictive features (genes) that will provide better insight into the biological mechanism at play in the host response to infections. To achieve this, we will regularize (1.1) with the ℓ_q -norm for $0 < q < 1$. This results in the minimization problems

$$\min_{\mathbf{z}_i \in \mathbb{R}^m} \frac{\|A_i \mathbf{z}_i\|_2^2}{\|A_j \mathbf{z}_i\|_2^2} + \delta_i \|\mathbf{z}_i\|_q^q, \quad i, j \in \{1, 2\}, \quad i \neq j, \quad 0 < q < 1, \quad (1.5)$$

where

$$\|\mathbf{y}\|_q = \left(\sum_{i=1}^m |y_i|^q \right)^{1/q}, \quad \mathbf{y} = [y_1, y_2, \dots, y_m]^T \in \mathbb{R}^m.$$

Unless otherwise stated, $|y|$ denotes the absolute value of $y \in \mathbb{R}$.

The quantity $\|\mathbf{y}\|_q$ is referred to as the ℓ_q -norm of \mathbf{y} . For $0 < q < 1$, the mapping $\mathbf{y} \mapsto \|\mathbf{y}\|_q$ is not a norm since the triangle inequality is not satisfied. Nevertheless, this is of interest since the ℓ_q -norm for $0 < q < 1$ tends to “shrink” entries of \mathbf{y} more rapidly to zero and can be more robust to outliers than the ℓ_1 -norm. We will refer to the minimization problems (1.5) as the ℓ_q -GSVP. The ℓ_q -GSVP allows for q to be flexibly adjusted to attain a desired sparsity level in the computed solutions. Thus, different levels of sparsity can be adapted to different datasets; see, e.g., [30, 29] for applications of ℓ_q -norm in a closely related context.

We note that the minimization problems (1.1) and (1.4) are *non-convex* optimization problems. While (1.1) is differentiable, its regularized counterparts in (1.4) and (1.5) are non-differentiable. This is due to the presence of ℓ_q penalty terms for $0 < q \leq 1$; see [32, 12] for related discussions when $q = 1$. The main drawback for $0 < q < 1$ is that the minimization problems (1.5) are purely non-convex, whereas (1.4) have both non-convex and convex parts. In these situations, our objective functions have differentiable and non-differentiable parts. Thus, optimization algorithms, such as Proximal Gradient Descent (PGD), can be applied to determine approximate solutions of (1.1) and (1.5) that are sparse; see, e.g., [23, 2] for discussions.

We remark that application of PGD to (1.4) and (1.5) provides the ℓ_1 -PGD-GSVP and ℓ_q -PGD-GSVP methods, respectively. In the ℓ_q -PGD-GSVP method, $\|\mathbf{z}_i\|_q^q$ is first approximated by a weighted ℓ_2 -norm, then the PGD algorithm applied to solve the resulting problems. Details of these methods will be provided in Sections 2 and 3.

Our major contributions in this paper are as follows:

1. We develop novel algorithms that apply the PGD to compute sparse generalized singular vectors associated with the smallest generalized singular values of the matrix pairs in (1.1). This leads to the ℓ_q -PGD-GSVP method for $0 < q \leq 1$.
2. We integrate Support Vector Machines [8, SVM] into the ℓ_q -PGD-GSVP framework to carry out dimensionality reduction and feature selection in high-dimensional feature space, such as gene expression dataset associated with ovarian cancer. The resulting sparse technique will be referred to as the ℓ_q -PGD-GSVPSVM method. We mention that SVM has a well-established history in the analysis of gene expression data; see, e.g., [15, 21, 10, 4], and the incorporation of SVM into the framework of (1.1) was first proposed in [19]; see Section 4 for details.
3. Finally, we discuss the binary classification of breast and ovarian cancer datasets described in Section 5, Table 1, with proximal SVM. The classification process uses a parsimonious set of features selected by the ℓ_1 -PGD-GSVPSVM and ℓ_q -PGD-GSVPSVM methods; see Algorithm 3. Different choices of q are adapted to select a broad range of features from each dataset. The $\ell_{0.1}$ -PGD-GSVPSVM method is quite competitive and results in 100% classification accuracy with ovarian cancer dataset. This result is consistent with the most recent baseline accuracy in the literature; see, e.g., [9]. Moreover, the superiority of $\ell_{0.1}$ -PGD-GSVPSVM method lies in its ability to select the least number of informative genes. Overall, our approaches are seen to handle imbalanced data effectively.

In the following subsection, we will explore relevant literature that focuses on the application of SVM in the context of (1.1).

1.1 A Review of Related Methods

To the best of our knowledge, we are the first to develop and apply the ℓ_q -PGD-GSVPSVM framework for the solutions of (1.4) and (1.5). However, the integration of SVM into the generalized Rayleigh quotients (1.1) is not new. The idea was first proposed in a seminal work by Mangasarian and Wild [19] and referred to as the Generalized Eigenvalue Proximal SVM (GEP SVM).

The GEP SVM regularizes the numerator of (1.1) with a squared ℓ_2 -norm. This shifts the spectrum of $A_i^T A_i$ in (1.3) by $\delta_i I$, where I is an identity matrix of compatible size. The solutions of the GEP SVM determine two non-parallel separating hyperplanes for binary classification tasks while the GEP SVM demands that each hyperplane be closest to the samples of one class and further from the samples of the other class. The classification of new input data depends on their proximity to either of the hyperplanes.

Several different formulations of the GEP SVM have been described in the literature; see, e.g., [30, 33, 18, 6, 32, 12, 28, 27] and references therein. In particular, the methods presented in [30, 33, 18] replace the ℓ_2 -norm in (1.1) with the ℓ_1 -norm, and solve the resulting minimization problems iteratively. These methods, commonly referred to as the Non-Parallel Proximal SVM (NPSVM), differ from the GEP SVM and the methods described in [6, 32, 12, 28, 27] since they do not involve solving a pair of generalized eigenvalue problems. While [18] does not employ regularization terms, [30] and [33] introduce ℓ_q -norm, $q > 0$, and ℓ_2 -norm regularization terms, respectively, in the numerator of the NPSVM formulation.

Yet another closely related approach, but again different from our ℓ_1 -GSVPSVM, is the Regularized Generalized Eigenvalue Classifier [13, ReGEC] with ℓ_1 -norm regularization, proposed and applied in [32, 12, ℓ_1 -ReGEC]. The ReGEC-type methods are analogous to the GEP SVM, in that, they handle singularity issues that may arise in (1.3), by shifting the spectrum of $A_i^T A_i$ and $A_j^T A_j$ by $\delta_i A_j^T A_j$ and $\delta_j A_i^T A_i$, respectively. One advantage of the ReGEC-type techniques over the GEP SVM is that only a single GEP needs to be solved to determine the two separating hyperplanes [13].

Differently from the ℓ_q -GSVPSVM, $0 < q \leq 1$, both the GEP SVM and NPSVM incorporate regularization terms into the numerator of their fidelity terms. Moreover, the practicability of the GEP SVM, NPSVM, and ReGEC approaches is significantly limited due to their enormous computational and memory requirements for large-scale problems. Specifically, their reliance on computing the generalized eigenvalue decomposition make them less attractive for large-scale problems, such as the ovarian cancer classification, where the number of columns, m , greatly exceeds the number of rows, ℓ and p ($m \gg \ell \geq p$). We remark that these methods have been seen to perform exceptionally well on small-size problems for which $\ell \geq p \gg m$. Additionally, the ℓ_1 -norm sparse method proposed in [25] for feature selection in high-dimensional datasets requires explicit computation of $A_1^T A_1$ and $A_2^T A_2$, as well as their Cholesky factorizations.

The organization of this paper is as follows. Section 2 provides an overview of the PGD algorithm and discusses how it can be applied to solve (1.4). This leads to the ℓ_1 -PGD-GSVP method. The ℓ_q -PGD-GSVP method for the solutions of (1.5) is presented in Section 3. This method requires approximating the ℓ_q -norm for $0 < q < 1$ by a weighted ℓ_2 -norm before applying the PGD algorithm. Section 4 focuses on the formulation of the ℓ_q -GSVPSVM for $0 < q \leq 1$ and outlines how the PGD algorithm is employed to derive the ℓ_q -PGD-GSVPSVM method. In Section 5, numerical experiments with the breast and ovarian cancer datasets are used to illustrate the performance of the proposed methods for $\ell \geq p \gg m$ and $m \gg \ell \geq p$, respectively. Section 6 presents concluding remarks.

2 The ℓ_1 -PGD-GSVP method for the solutions of (1.4)

This section discusses the solution method for (1.4) by applying the Proximal Gradient Descent [23, PGD] algorithm, and will be referred to as the ℓ_1 -PGD-GSVP method. We begin by briefly reviewing the PGD algorithm.

The PGD algorithm can be applied to solve minimization problems of the form

$$\min_{\mathbf{z} \in \mathbb{R}^m} r(\mathbf{z}) + g(\mathbf{z}),$$

where $r : \mathbb{R}^m \rightarrow \mathbb{R}$ is a smooth (convex) function that is differentiable and $g : \mathbb{R}^m \rightarrow \mathbb{R}$ is a nonsmooth (convex) function that typically incorporates a regularization term. The PGD algorithm iteratively alternates between the Gradient Descent (GD) and the proximal steps.

The GD step at the k th iteration is given by

$$\mathbf{y}^{(k)} = \mathbf{z}^{(k)} - \alpha \nabla r(\mathbf{z}^{(k)}), \quad (2.6)$$

where $\alpha > 0$ is a step size that can be fixed or determined at each iteration using the *backtracking* technique; see, e.g., [23, pg. 148] for discussion. The quantity $\nabla r(\mathbf{z}^{(k)})$ is the gradient of r at $\mathbf{z}^{(k)}$. The PGD algorithm computes the gradient of r at each iteration, takes a step in the direction of the steepest descent, which is given by $-\nabla r(\mathbf{z}^{(k)})$, then applies the proximal operator, denoted by $\mathbf{z}^{(k+1)} := \mathbf{prox}_{\alpha g}(\mathbf{y}^{(k)})$, to each iterate $\mathbf{y}^{(k)}$, in order to integrate the non-smooth function g into the optimization process. The proximal operator is defined by

$$\mathbf{prox}_{\alpha g}(\mathbf{y}^{(k)}) := \underset{\mathbf{z}}{\operatorname{argmin}} \left\{ \|\mathbf{z} - \mathbf{y}^{(k)}\|_2^2 + g(\mathbf{z}) \right\}. \quad (2.7)$$

The goal of the proximal step (2.7) is to determine a new point $\mathbf{z}^{(k+1)}$ that is “close” to $\mathbf{y}^{(k)}$. The PGD algorithm continues to iterate between the GD and proximal steps until a set convergence criterion is met. A notable property of the proximal operator is that \mathbf{z}^* is a minimizer of r if and only if $\mathbf{z}^* = \mathbf{prox}_{\alpha g}(\mathbf{z}^*)$.

For the minimization problems in (1.4), we let $h(\mathbf{z}_i) = r(\mathbf{z}_i) + g(\mathbf{z}_i)$, where

$$r(\mathbf{z}_i) = \frac{\|A_i \mathbf{z}_i\|_2^2}{\|A_j \mathbf{z}_i\|_2^2}, \quad \text{and} \quad g(\mathbf{z}_i) = \delta_i \|\mathbf{z}_i\|_1, \quad i, j \in \{1, 2\}, \quad i \neq j.$$

Since r is differentiable, its gradient is given by

$$\nabla r(\mathbf{z}_i^{(k)}) = \frac{2}{\|A_j \mathbf{z}_i^{(k)}\|_2^2} \left(A_i^T (A_i \mathbf{z}_i^{(k)}) - r(\mathbf{z}_i^{(k)}) A_j^T (A_j \mathbf{z}_i^{(k)}) \right), \quad i, j \in \{1, 2\}, \quad i \neq j. \quad (2.8)$$

Hence, the GD step (2.6) is expressed as

$$\mathbf{y}_i^{(k)} = \mathbf{z}_i^{(k)} - \alpha \nabla r(\mathbf{z}_i^{(k)}), \quad i = 1, 2. \quad (2.9)$$

The proximal operator that is associated with $g(\mathbf{z}_i) = \delta_i \|\mathbf{z}_i\|_1$ is readily expressed as a soft-thresholding operator. To see this, consider the explicit form of (2.7) with $g(\mathbf{z}_i) = \delta_i \|\mathbf{z}_i\|_1$. Then

$$\mathbf{prox}_{\alpha g}(\mathbf{y}_i^{(k)}) = \underset{z_i}{\operatorname{argmin}} \left\{ \sum_{l=1}^m (z_{il} - y_{il}^{(k)})^2 + \alpha \delta_i |z_{il}| \right\}, \quad (2.10)$$

where we denote $\mathbf{x}_i \in \mathbb{R}^m$ as $\mathbf{x}_i := [x_{i1}, x_{i2}, \dots, x_{im}]^T$, $l = 1, 2, \dots, m$. Let

$$f(z_{il}) = \sum_{l=1}^m (z_{il} - y_{il}^{(k)})^2 + \alpha \delta_i |z_{il}| = \sum_{l=1}^m (z_{il} - y_{il}^{(k)})^2 + \alpha \delta_i \operatorname{sign}(z_{il}) z_{il},$$

where $\operatorname{sign}(\cdot)$ is the sign operator. Taking element-wise partial derivative of f with respect to $z_{il} > 0$ and $z_{il} < 0$, and setting the results to zero gives

$$z_{il} > 0: \quad z_{il} = y_{il}^{(k)} - \frac{\alpha \delta_i}{2}, \quad \text{and} \quad z_{il} < 0: \quad z_{il} = y_{il}^{(k)} + \frac{\alpha \delta_i}{2}.$$

Thus,

$$z_{il} = \begin{cases} y_{il}^{(k)} + \frac{\alpha \delta_i}{2}, & y_{il}^{(k)} < -\frac{\alpha \delta_i}{2}, \\ 0 & -\frac{\alpha \delta_i}{2} \leq y_{il}^{(k)} \leq \frac{\alpha \delta_i}{2}, \\ y_{il}^{(k)} - \frac{\alpha \delta_i}{2}, & y_{il}^{(k)} > \frac{\alpha \delta_i}{2}. \end{cases} \quad (2.11)$$

Equation (2.11) is a piece-wise representation of z_{il} in terms of $y_{il}^{(k)}$, and it leads to the soft-thresholding operator

$$\mathbf{z}_i^{(k+1)} = \operatorname{sign}(\mathbf{y}_i^{(k)}) \cdot \max \left(|\mathbf{y}_i^{(k)}| - \frac{\alpha \delta_i}{2}, 0 \right), \quad i = 1, 2, \quad (2.12)$$

where \cdot denotes the usual scalar multiplication.

The solution method so described is the ℓ_1 -PGD-GSVP method. Its implementation is carried out by Algorithm 1. Lines 6 and 7 of this algorithm represent updates for the GD and proximal steps, respectively. Notice that the ℓ_1 -PGD-GSVP algorithm avoids explicit formation of $A_1^T A_1$ and $A_2^T A_2$ at each iteration to enhance computational efficiency and minimize storage requirements.

Algorithm 1: The ℓ_1 -PGD-GSVP method for the solution of (1.4)

Input: $A_1 \in \mathbb{R}^{\ell \times m}$, $A_2 \in \mathbb{R}^{\ell \times m}$, $\alpha > 0$, \maxiter , $\delta_1 > 0$, $\delta_2 > 0$, $\mathbf{z}_1^{(0)}$, $\mathbf{z}_2^{(0)}$

1 **for** $k = 1 : \maxiter$ **do**

2 $k := k - 1$

3 Compute $r(\mathbf{z}_i^{(k)}) = \frac{(A_i \mathbf{z}_i^{(k)})^T A_i \mathbf{z}_i^{(k)}}{(A_j \mathbf{z}_i^{(k)})^T A_j \mathbf{z}_i^{(k)}}$, $i, j \in \{1, 2\}$, $i \neq j$ (2.13)

4 Compute $\nabla r(\mathbf{z}_i^{(k)})$ by using (2.8)

5 Compute $\mathbf{y}_i^{(k)}$ by using (2.9)

6 Update $\mathbf{z}_i^{(k+1)}$ by using (2.12)

7 **if** $\frac{\|h(\mathbf{z}_i^{(k+1)}) - h(\mathbf{z}_i^{(k)})\|_2}{\|h(\mathbf{z}_i^{(k)})\|_2} < 10^{-4}$ **then**

8 | break

9 **end**

10 **end**

3 The ℓ_q -PGD-GSVP, $0 < q < 1$, method for the solutions of (1.5)

This section describes the ℓ_q -PGD-GSVP method for the solution of non-convex minimization problems (1.5). Our strategy is to first transform (1.5) into equivalent differentiable problems by approximating the ℓ_q -norm with a weighted ℓ_2 -norm. Thereafter, apply the PGD algorithm to solve the resulting problems. The use of weighted ℓ_2 -norm to approximate ℓ_q -norm for $0 < q \leq 1$ is quite ubiquitous in the literature. Refer to [34] for a recent discussion on the proximal operator of the ℓ_q -norm for $0 \leq q < 1$.

Let $\mathbf{z}_i = [z_{i_1}, z_{i_2}, \dots, z_{i_m}]^T$, and define $\phi_\epsilon(z_{i_k}) := (z_{i_k}^2 + \epsilon^2)^{\frac{1}{2}}$ for $\epsilon > 0$. Then

$$\|\mathbf{z}_i\|_q^q \approx \sum_{k=1}^m (z_{i_k}^2 + \epsilon^2)^{(q-2)/2} z_{i_k}^2 = \mathbf{z}_i^T \left(\sum_{k=1}^m \phi_\epsilon(z_{i_k})^{(q-2)} \right) \mathbf{z}_i = \mathbf{z}_i^T D_{\epsilon, q}(\mathbf{z}_i) \mathbf{z}_i = \|D_{\epsilon, q}^{\frac{1}{2}}(\mathbf{z}_i) \mathbf{z}_i\|_2^2, \quad (3.14)$$

where

$$D_{\epsilon, q}(\mathbf{z}_i) = \text{diag} \left(\phi_\epsilon(z_{i_1})^{(q-2)}, \phi_\epsilon(z_{i_2})^{(q-2)}, \dots, \phi_\epsilon(z_{i_m})^{(q-2)} \right) \in \mathbb{R}^{m \times m}. \quad (3.15)$$

Substitution of (3.14) into (1.5) yields the transformed ℓ_q -regularized problems

$$\min_{\mathbf{z}_i \in \mathbb{R}^m} \frac{\|A_i \mathbf{z}_i\|_2^2}{\|A_j \mathbf{z}_i\|_2^2} + \delta_i \|D_{\epsilon, q}^{\frac{1}{2}}(\mathbf{z}_i) \mathbf{z}_i\|_2^2, \quad i, j \in \{1, 2\}, \quad i \neq j, \quad 0 < q < 1. \quad (3.16)$$

The minimization problems (3.16) are the equivalent versions of (1.5) that are differentiable with convex regularization parts. We will follow a similar approach described in Section 2 to derive the ℓ_q -PGD-GSVP method. Here, only the derivation of the proximal step of the ℓ_q -PGD-GSVP method will be presented while the GD step is given by (2.9).

For a given point $\mathbf{z}_i^{(k)}$, let $g(\mathbf{z}_i) = \delta_i \|D_{\epsilon, q}^{\frac{1}{2}}(\mathbf{z}_i^{(k)}) \mathbf{z}_i\|_2^2$. Then the approximate solutions of (3.16) can be computed as

$$\mathbf{z}_i^{(k+1)} = \underset{\mathbf{z}_i \in \mathbb{R}^m}{\text{argmin}} \left\{ \|\mathbf{z}_i - \mathbf{y}_i^{(k)}\|_2^2 + \alpha \delta_i \|D_{\epsilon, q}^{\frac{1}{2}}(\mathbf{z}_i^{(k)}) \mathbf{z}_i\|_2^2 \right\}, \quad i = 1, 2.$$

Let $s(\mathbf{z}_i) = \|\mathbf{z}_i - \mathbf{y}_i^{(k)}\|_2^2 + \alpha \delta_i \|D_{\epsilon, q}^{\frac{1}{2}}(\mathbf{z}_i^{(k)}) \mathbf{z}_i\|_2^2$. Computing the gradient of s with respect to \mathbf{z}_i and setting the results to zero provides the following update rule for the proximal step:

$$\mathbf{z}_i^{(k+1)} = (I + \alpha \delta_i D_{\epsilon, q}(\mathbf{z}_i^{(k)}))^{-1} \mathbf{y}_i^{(k)}, \quad i = 1, 2. \quad (3.17)$$

Equation (3.17) represent the proximal steps of the ℓ_q -PGD-GSVP method, which is described by Algorithm 2 below. In our implementation of Algorithm 2, the diagonal matrices $(I + \alpha\delta_i D_{\epsilon,q}(\mathbf{z}_i^{(k)}))$ and their inverses are not formed or computed explicitly. Rather, (3.17) are cheaply computed as element-wise products of two vectors.

Algorithm 2: The ℓ_q -PGD-GSVP method for the solution of (1.5)

Input: $A_1 \in \mathbb{R}^{\ell \times m}$, $A_2 \in \mathbb{R}^{\ell \times m}$, $\alpha > 0$, maxiter, $\delta_1 > 0$, $\delta_2 > 0$, $\mathbf{z}_1^{(0)}$, $\mathbf{z}_2^{(0)}$

```

1 for  $k = 1$  : maxiter do
2    $k := k - 1$ 
3   Compute  $D_{\epsilon,q}(\mathbf{z}_i^{(k)})$  by using (3.15)
4   Compute  $r(\mathbf{z}_i^{(k)})$  by using (2.13)
5   Compute  $\nabla r(\mathbf{z}_i^{(k)})$  by using (2.8)
6   Compute  $\mathbf{y}_i^{(k)}$  by using (2.9)
7   Update  $\mathbf{z}_i^{(k+1)}$  by using (3.17)
8   if  $\frac{\|h(\mathbf{z}_i^{(k+1)}) - h(\mathbf{z}_i^{(k)})\|_2}{\|h(\mathbf{z}_i^{(k)})\|_2} < 10^{-4}$  then
9     | break
10  end
11 end

```

4 The ℓ_q -GSVPSVM for $0 < q \leq 1$

This section describes the integration of the SVM framework into the ℓ_q -GSVP for $0 < q \leq 1$ (cf. (1.4) and (1.5)). The resulting problems will be referred to as the ℓ_q -GSVPSVM, $0 < q \leq 1$, where $q = 1$ refers to both weighted and unweighted ℓ_1 penalty.

Let $A_1 \in \mathbb{R}^{\ell \times m}$ represent a training dataset of interest with n_1 (Class 0) samples, and n_2 (Class 1) samples, in that order, such that $\ell = n_1 + n_2$. Suppose the class matrices, $C_1 \in \mathbb{R}^{n_1 \times m}$ and $C_2 \in \mathbb{R}^{n_2 \times m}$, represent all the training data points from A_1 that correspond to Class 0 and Class 1, respectively.

Also, let

$$\tilde{C}_1 := [C_1 \mathbf{e}_1] \in \mathbb{R}^{n_1 \times (m+1)} \quad \text{and} \quad \tilde{C}_2 := [C_2 \mathbf{e}_2] \in \mathbb{R}^{n_2 \times (m+1)}, \quad (4.18)$$

where $\mathbf{e}_1 \in \mathbb{R}^{n_1}$ and $\mathbf{e}_2 \in \mathbb{R}^{n_2}$ are vectors of ones. Then the ℓ_q -GSVPSVM for $0 < q \leq 1$ can be formulated as

$$\min_{\tilde{\mathbf{w}}_i \in \mathbb{R}^m} \frac{\|\tilde{C}_i \tilde{\mathbf{w}}_i\|_2^2}{\|\tilde{C}_j \tilde{\mathbf{w}}_i\|_2^2} + \delta_i \|\tilde{\mathbf{w}}_i\|_q^q, \quad i, j \in \{1, 2\}, \quad i \neq j, \quad 0 < q \leq 1. \quad (4.19)$$

Notably, the use of the ℓ_q penalty in (4.19) distinguishes our work from [19] and others described in the literature. The vectors $\tilde{\mathbf{w}}_1$ and $\tilde{\mathbf{w}}_2$ determine two non-parallel separating hyperplanes:

$$\mathbf{x}^T \mathbf{w}_1 + b_1 = 0, \quad \text{and} \quad \mathbf{x}^T \mathbf{w}_2 + b_2 = 0, \quad \mathbf{w}_1, \mathbf{w}_2 \in \mathbb{R}^m, \quad (4.20)$$

where $b_1, b_2 \in \mathbb{R}$ are the *bias* terms; and the vectors \mathbf{w}_1 and \mathbf{w}_2 represent the normal to their respective hyperplane. The first hyperplane in (4.20) is closest to the samples of Class 0 and furthest from the samples of Class 1 while the second hyperplane is closest to the samples of Class 1 and furthest from the samples of Class 0. We will apply the PGD algorithm to solve the ℓ_q -GSVPSVM (4.19). This leads to the ℓ_q -PGD-GSVPSVM methods, for $0 < q \leq 1$. The performance of these methods will be illustrated in Section 5. Note that when Algorithm 1 is employed to compute the solutions of (4.19) for $q = 1$, we will refer to the resulting method as the ℓ_1 -PGD-GSVPSVM method.

Analogously to [30, 33, 18, 6, 19, 13, 32, 12, 28, 27], we will utilize \mathbf{w}_1 and \mathbf{w}_2 to define a proximal classifier that exploits the sparsity levels in both weights to carry out feature selection and binary classification. Specifically, \mathbf{w}_1 and \mathbf{w}_2 are first arranged in descending order of magnitude to obtain the vectors $\hat{\mathbf{w}}_1$ and $\hat{\mathbf{w}}_2$. The near-zero coefficients of $\hat{\mathbf{w}}_1$ and $\hat{\mathbf{w}}_2$ correspond to the less informative features, while the most significant non-zero elements indicate more relevant features.

Once the most relevant features have been identified, a proximal SVM classifier is employed for binary classification. A new sample point \mathbf{x} is classified to either Class 1 or Class 0 by using

$$\text{Class}(\mathbf{x}) := \begin{cases} 0 & \text{if } \frac{|\mathbf{x}^T \mathbf{w}_1 + b_1|}{\|\mathbf{w}_1\|_2} \leq \frac{|\mathbf{x}^T \mathbf{w}_2 + b_2|}{\|\mathbf{w}_2\|_2} \\ 1 & \text{if otherwise.} \end{cases} \quad (4.21)$$

Note that the non-zero coefficients of $\hat{\mathbf{w}}_1$ and $\hat{\mathbf{w}}_2$ with the highest magnitude correspond to the top features in C_1 and C_2 , while features that are associated with the near-zero coefficients of $\hat{\mathbf{w}}_1$ and $\hat{\mathbf{w}}_2$ are discarded. This process of eliminating the less informative features leads to reduction in dimensions of the feature spaces of C_1 and C_2 . The entire procedure so described is summarized by Algorithm 3 below.

Algorithm 3: The ℓ_q -PGD-GSVPSVM, $0 < q \leq 1$, method for feature selection and binary classification

- Input:** $A_1 := \begin{bmatrix} C_1 \\ C_2 \end{bmatrix}$, $A_2 := \begin{bmatrix} \hat{C}_1 \\ \hat{C}_2 \end{bmatrix}$, where $C_i \in \mathbb{R}^{n_i \times m}$ and $\hat{C}_i \in \mathbb{R}^{\hat{n}_i \times m}$, $i = 1, 2$, are class matrices, and A_1 and A_2 are the training and validation data matrices. n_i , \hat{n}_i denote the number of class samples, and m is the number of features in each class
- 1 Solve the minimization problems (4.19) for $\tilde{\mathbf{w}}_1$ and $\tilde{\mathbf{w}}_2$ by using Algorithms 1 and 2, respectively, with $\tilde{C}_1 \in \mathbb{R}^{n_1 \times (m+1)}$ and $\tilde{C}_2 \in \mathbb{R}^{n_2 \times (m+1)}$ defined by (4.18)
 - 2 Set $\tilde{\mathbf{w}}_1 := [\mathbf{w}_1^T \ b_1]^T$ and $\tilde{\mathbf{w}}_2 := [\mathbf{w}_2^T \ b_2]^T$
 - 3 Sort \mathbf{w}_1 and \mathbf{w}_2 in descending order of magnitude, and denote the sorted analogues as $\hat{\mathbf{w}}_1$ and $\hat{\mathbf{w}}_2$. Let the rank indices associated with $\hat{\mathbf{w}}_1$ and $\hat{\mathbf{w}}_2$ be denoted by R_1 and R_2 , respectively
 - 4 Plot $\hat{\mathbf{w}}_1$ and $\hat{\mathbf{w}}_2$ on the same graph to determine the elbow points, (x_1, y_1) and (x_2, y_2) , respectively
 - 5 Denote the first x_1 and x_2 indices in R_1 and R_2 as $R_1(x_1)$ and $R_2(x_2)$, respectively
 - 6 Set entries of \mathbf{w}_1 and \mathbf{w}_2 to zero if that do not have corresponding indices in $R_1(x_1)$ and $R_2(x_2)$, respectively
 - 7 Use (4.21) to classify the samples in A_2
-

5 Numerical Experiments

In this section, all computations are carried out on a Dell computer running Windows 11 with 13th Gen Intel(R) Core(TM) i9-13900H @ 2.60GHz and 64 GB RAM. The ℓ_q -PGD-GSVPSVM methods are implemented and analyzed using Jupyter Notebook running on VSCode. For reproducibility of the results presented herein, we set `random_state = 42`. The implementation of the methods can be found <https://github.com/Obinnah/Sparse-GSVP/blob/main/gsvp/demos/gsvp-demo.ipynb>

We will compute sparse solutions of the ℓ_q -GSVPSVM (cf. (4.19)) by applying Algorithms 1 and 2. Then utilize the computed solutions for feature selection and binary classification purposes.

5.1 Datasets

The performance of the ℓ_q -PGD-GSVPSVM, $0 < q \leq 1$, methods for $\ell \gg m$ and $m \gg \ell$ will be examined using the *Breast Cancer* and *Ovarian Cancer* datasets, respectively.

The breast cancer dataset has fewer attributes than observations, and thus, corresponds to the situation where $\ell \gg m$, i.e., there are far more samples ℓ than features m . For this dataset, we will focus on accurately classifying benign and malignant breast cancer subjects.

The ovarian cancer dataset consists of transcriptional gene expression from ovarian cancer screening. This dataset has significantly more genes m than samples ℓ , i.e., $m \gg \ell$, and it involves classifying normal and cancer subjects. While the breast cancer dataset can be found on www.kaggle.com, the ovarian cancer dataset can be downloaded from <https://csse.szu.edu.cn/staff/zhuzx/Datasets.Html>.

Table 1 presents a detailed description of the datasets, highlighting random splits of the class samples. Specifically, 70% of the class samples are used for training, and the remaining 30% are

Dataset	Size ($\ell \times m$)	Class	Training Samples	Validation Samples	Test Samples
Breast Cancer	569×30	Benign	249	64	44
		Malignant	148	38	26
Ovarian Cancer	253×15154	Normal	63	19	9
		Cancer	113	34	15

Table 1: Description of the datasets for numerical experiments

split into validation and test sets in the ratio of 60 : 40 for the breast cancer dataset and 70 : 30 for the ovarian cancer dataset. The validation set is used to determine the model parameters below.

5.2 Evaluation Metrics

The evaluation metric for the ℓ_q -PGD-GSVPSVM methods is the Balanced Accuracy (Bal. Acc.). This metric is well-suited for datasets with imbalanced classes and is defined by

$$\text{Balanced Accuracy} := \frac{1}{2} \left(\frac{TP}{TP + FN} + \frac{TN}{TN + FP} \right) = \frac{\text{Recall} + \text{Specificity}}{2},$$

where the True Negative (TN) represents the number of C_1 or \hat{C}_1 (cf. Algorithm 3) samples that are correctly classified, and True Positive (TP) represents the number of C_2 or \hat{C}_2 (cf. Algorithm 3) samples that are correctly classified. Furthermore, False Positive (FP) corresponds to the number of incorrectly classified C_1 or \hat{C}_1 samples, while False Negative (FN) denotes the number of incorrectly classified C_2 or \hat{C}_2 samples. Note that

$$\text{Precision} := \frac{TP}{TP + FP}$$

To measure the stability of the selected set of features across different q , we compute the Avg. Jaccard Similarity Index (JSI), where for any two sets S_1 and S_2 , the JSI is defined as

$$\text{JSI}(S_1, S_2) := \frac{|S_1 \cap S_2|}{|S_1 \cup S_2|},$$

where $|S|$ denotes the cardinality of a set S . Define $\mathcal{S}_q := \{S_1, S_2, \dots, S_N\}$, and let the subsets S_i , $i = 1, 2, \dots, N$, denote the set of features selected for each q . Then the Avg. JSI is given by

$$\frac{\text{Total JSI}}{\binom{N}{2}} = \frac{2 \sum_{1 \leq i, j \leq N} \text{JSI}(S_i, S_j)}{(N-2)!}, \quad i \neq j.$$

An Avg. JSI of 1 indicates strong similarity among the subsets of features associated with each q . However, an Avg. JSI close to zero indicates weak similarity among subsets of features in \mathcal{S}_q .

5.3 Model Parameters

Unless otherwise stated, the model parameters for the ℓ_1 -PGD-GSVPSVM, and ℓ_q -PGD-GSVPSVM, $0 < q \leq 1$, methods are as follows:

1. The algorithms are terminated once a set convergence criterion (cf. step 8, Algorithm 1) is met or the maximum number of iterations (`maxiter`) is reached. Here, we set `maxiter` = 10,000 and remark that the `maxiter` can affect the accuracy of the methods as well as the number of features selected.
2. The regularization parameters, δ_1 and δ_2 , are determined using grid search over the intervals $[10^{-4}, 1]$ and $[2 \cdot 10^{-4}, 1]$, respectively.
3. The step size, α , is determined using grid search over the set

$$\beta \cdot \{10^{-0.5}, 10^{-1}, 10^{-1.5}, 10^{-2}, 10^{-2.5}, 10^{-3}, 10^{-3.5}\}, \quad \beta > 0.$$

Table 2 shows the model parameters determined for the ℓ_q -PGD-GSVPSVM methods. The best parameters are expected to result in sparse solutions, i.e., solutions with steep slopes characterized by non-oscillating objective function values and relative errors (cf. Figure 1 below). Generally, the methods drive the solutions to near zero, but the induced sparsity level and the observed steep slopes may depend on q and other parameters, such as ϵ , step size, and `maxiter`. Below, we examine the sensitivity of the computed solutions to q and ϵ using the ovarian cancer dataset.

Method	Dataset	δ_1	δ_2	α
ℓ_1 -PGD-GSVPSVM	Breast Cancer	$\frac{20627}{23750}$	$\frac{20627}{23750}$	10^{-3}
	Ovarian Cancer	$\frac{2259}{47500}$	$\frac{2259}{47500}$	$4 \cdot 10^{-3}$
ℓ_q -PGD-GSVPSVM, $q = 1$	Breast Cancer	$3 \cdot 10^{-1}$	$4 \cdot 10^{-1}$	$3 \cdot 10^{-3}$
	Ovarian Cancer	$3 \cdot 10^{-3}$	$3 \cdot 10^{-3}$	$10^{-0.5}$
$\ell_{0.1}$ -PGD-GSVPSVM	Breast Cancer	$2 \cdot 10^{-2}$	$2 \cdot 10^{-2}$	$2.5 \cdot 10^{-3}$
	Ovarian Cancer	$6 \cdot 10^{-2}$	$6 \cdot 10^{-2}$	$10^{-0.5}$

Table 2: Model parameters.

5.4 The Sensitivity of the Solutions to q

Consider $q := \{0.1, 0.2, 0.3, 0.4, 0.5, 0.6, 0.7, 0.8, 0.9, 1\}$ and take $\epsilon = 10^{-2.5}$. We demonstrate with the ovarian cancer dataset that smaller values of q often result in sparser solutions than larger values of q . Specifically, Figure 1 shows that the solutions determined by the ℓ_q -PGD-GSVPSVM method for $q = 0.2$ have steeper slopes than those of $q = 0.9$. This behavior is consistent with other values of q . Analogously, Figure 2 shows that the ℓ_1 -PGD-GSVPSVM method also promote sparsity in the computed solutions.

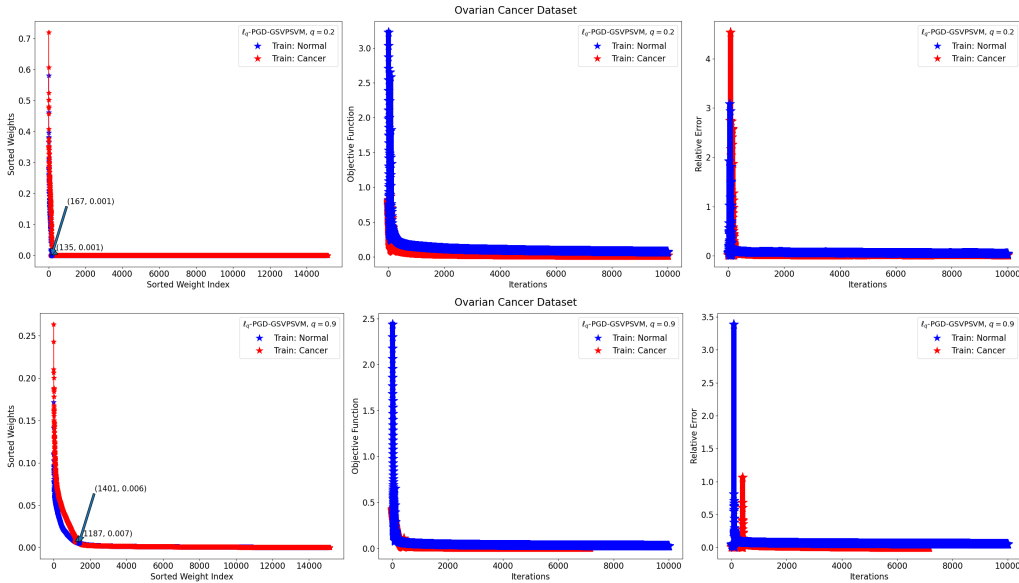


Figure 1: The ℓ_q -PGD-GSVPSVM method yields sparser solutions for $q = 0.2$ than $q = 0.9$.

5.5 The Sensitivity of Feature Selection to q and ϵ

The feature selection process is delineated in steps 3-6 of Algorithm 3. This process proceeds by first sorting the weights, \mathbf{w}_1 and \mathbf{w}_2 , in descending order of magnitude, then subsequently, plots

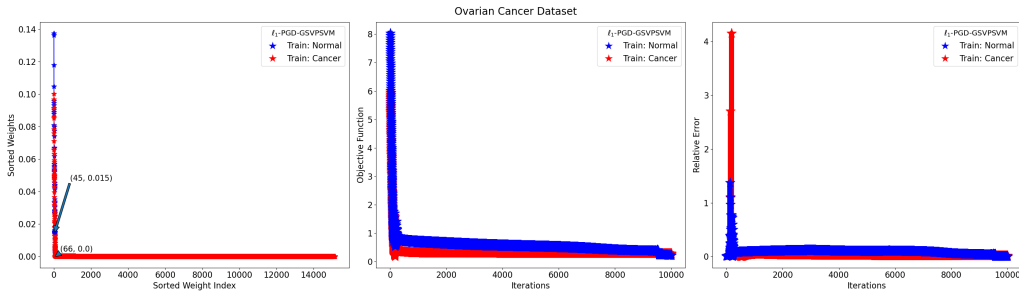


Figure 2: The ℓ_1 -PGD-GSVPSVM method promote sparsity in the computed solutions.

the sorted weights to identify the elbow points, as depicted in Figures 1 and 2. A python library called `Knee Finder`¹ is employed to determine the elbow points. The determined elbow points in Figures 1 and 2, represent the maximum distance from a line that connects the first and last points of each curve. The number of informative features selected for each q , corresponds to the smallest x -coordinate of the elbow points.

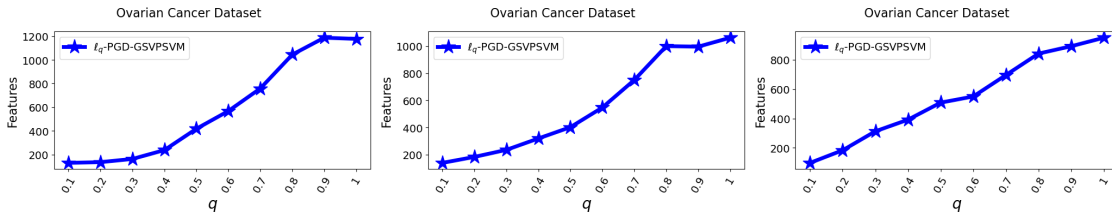


Figure 3: The number of features selected for different q values with $\epsilon = 10^{-2.5}$ (left), $\epsilon = 10^{-2}$ (middle) and $\epsilon = 10^{-1.5}$ (right).

Figure 3 shows that the smaller the q , the smaller the number of features (genes) selected. This trend is consistent across different choices of ϵ considered in Figure 3. Moreover, larger ϵ values tend to result in fewer number of features than smaller ϵ values. We report Avg. JSI of 0.6976, 0.6303, and 0.4260 for the ℓ_q -PGD-GSVPSVM, $0 < q \leq 1$, method with $\epsilon = 10^{-1.5}$, $\epsilon = 10^{-2}$, and $\epsilon = 10^{-2.5}$, respectively. These results suggest that the selected features across different q exhibit greater similarity when $\epsilon = 10^{-1.5}$ is used, compared to $\epsilon = 10^{-2}$ and $\epsilon = 10^{-2.5}$.

5.6 Model Performance on Sequestered Test Set

We examine the performance of the ℓ_1 -PGD-GSVPSVM, and ℓ_q -PGD-GSVPSVM, $0 < q \leq 1$, methods for $\ell \gg m$ and $m \gg \ell$. For simplicity, we consider $q = 0.1$ and $q = 1$ for weighted and unweighted ℓ_1 penalty. The training and validation processes are carried out by Algorithm 3, alongside Algorithms 1 and 2, respectively.

5.6.1 Case 1: $\ell \gg m$

We analyze the breast cancer dataset, which contains more samples ℓ than features m . Figure 4 illustrates that the weights determined by the $\ell_{0.1}$ -PGD-GSVPSVM method are sparse. Table 3 presents the elbow points and selected features corresponding to the ℓ_1 -PGD-GSVPSVM and ℓ_q -PGD-GSVPSVM ($q = 0.1$ and $q = 1$) methods. These methods select 7, 8 and 10 unique features, respectively. The selected features include those determined to be exclusive and common to the weights, \mathbf{w}_1 and \mathbf{w}_2 . For the breast cancer dataset, the elbow points of \mathbf{w}_1 and \mathbf{w}_2 identify the most significant features for the benign and malignant cancer classes, respectively.

The most informative features corresponding to both classes are displayed in Figure 5 for the ℓ_1 -PGD-GSVPSVM, $\ell_{0.1}$ -PGD-GSVPSVM, and ℓ_q -PGD-GSVPSVM ($q = 1$) methods. The selected features in Figure 5, with the exclusion of `smoothness_worst` and `area_se`, are subsets of the 18 most significant features for breast cancer diagnosis presented in [20] using a modified recursive

¹<https://pypi.org/project/kneefinder/>

feature elimination approach. Using 18 features, [20] achieved a 99% classification accuracy, and with only 7 features, they achieved 96% accuracy.

Table 4 presents the classification results for the breast cancer dataset on a sequestered test set. The ℓ_1 -PGD-GSVPSVM method yields a balanced accuracy of 96.15% with only 7 features, which is 1.13% higher than those of the ℓ_q -PGD-GSVPSVM method for $q = 0.1$ and $q = 1$.

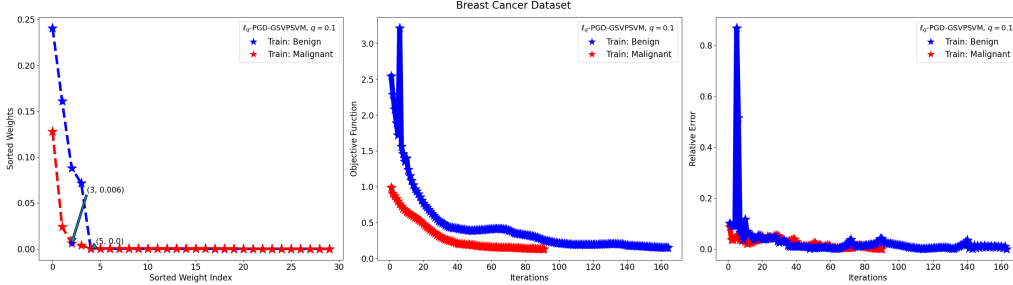


Figure 4: The solutions of the ℓ_q -PGD-GSVPSVM method for $q = 0.1$.

Dataset	Methods	Elbow Points		Features Selected		
		w_1	w_2	w_1 (Excl.)	w_2 (Excl.)	w_1/w_2 (Common)
Breast Cancer	ℓ_1 -PGD-GSVPSVM	4	4	3	3	1
	ℓ_q -PGD-GSVPSVM ($q = 1$)	7	3	7	3	0
	$\ell_{0.1}$ -PGD-GSVPSVM	5	3	5	3	0
Ovarian Cancer	ℓ_1 -PGD-GSVPSVM	67	42	60	35	7
	ℓ_q -PGD-GSVPSVM ($q = 1$)	101	94	83	76	18
	$\ell_{0.1}$ -PGD-GSVPSVM	2	2	2	2	0

Table 3: The elbow points and features selected by the weights of the ℓ_1 -PGD-GSVPSVM, and ℓ_q -PGD-GSVPSVM methods for $q = 0.1$ and $q = 1$.

Dataset	Methods	Bal. Acc.	Specificity	Recall	Precision	TN	FP	FN	TP
Breast Cancer (Validation)	ℓ_1 -PGD-GSVPSVM	98.68	100	97.37	100	64	0	1	37
	ℓ_q -PGD-GSVPSVM ($q = 1$)	98.68	100	97.37	100	64	0	1	37
	$\ell_{0.1}$ -PGD-GSVPSVM	96.59	98.44	94.74	97.30	63	1	2	36
Breast Cancer (Test)	ℓ_1 -PGD-GSVPSVM	96.15	100	92.31	100	44	0	2	24
	ℓ_q -PGD-GSVPSVM ($q = 1$)	95.02	97.73	92.31	96.00	43	1	2	24
	$\ell_{0.1}$ -PGD-GSVPSVM	95.02	97.73	92.31	96.00	43	1	2	24

Table 4: Classification reports for breast cancer dataset.

5.6.2 Case 2: $m \gg \ell$

Here, we demonstrate the effectiveness of the ℓ_1 -PGD-GSVPSVM, $\ell_{0.1}$ -PGD-GSVPSVM, and ℓ_q -PGD-GSVPSVM ($q = 1$) methods on ovarian cancer dataset, which has significantly more genes m than samples ℓ .

Figure 6 illustrates that weights determined by these methods are sparse, with the $\ell_{0.1}$ -PGD-GSVPSVM method resulting in sparser weights than the other methods considered. Table 3 shows that the $\ell_{0.1}$ -PGD-GSVPSVM method selects 4 genes while ℓ_1 -PGD-GSVPSVM and ℓ_q -PGD-GSVPSVM ($q = 1$) methods yield 102 and 177 informative genes, respectively. The most significant genes selected by these methods are displayed in Figure 7. Among the top 20 genes selected by the ℓ_1 -PGD-GSVPSVM and ℓ_q -PGD-GSVPSVM ($q = 1$) methods, 14 genes are consistent with the top genes selected in [9] by using filter-based methods, namely, chi-squared, F-statistic, and mutual information.

The last two columns of Figure 6 illustrate the discriminating power of the selected features. The fourth column of Figure 6 shows the two-dimensional Principal Component Analysis [17, PCA] embedding of the ovarian cancer dataset using all the genes. The PC plots with the selected genes

Feature Index (Normal)	Top Features (Normal)	Feature Index (Cancer)	Top Features (Cancer)	
0	12	perimeter_se	27	concave points_worst
1	7	concave points_mean	21	texture_worst
2	17	concave points_se	9	fractal_dimension_mean
3	23	area_worst	17	concave points_se
Feature Index (Benign)	Top Features (Benign)	Feature Index (Malignant)	Top Features (Malignant)	
0	12	perimeter_se	27	concave points_worst
1	7	concave points_mean	9	fractal_dimension_mean
2	2	perimeter_mean	21	texture_worst
3	3	area_mean		
4	17	concave points_se		
Feature Index (Benign)	Top Features (Benign)	Feature Index (Malignant)	Top Features (Malignant)	
0	12	perimeter_se	27	concave points_worst
1	7	concave points_mean	21	texture_worst
2	17	concave points_se	0	radius_mean
3	13	area_se		
4	23	area_worst		
5	3	area_mean		
6	24	smoothness_worst		

Figure 5: Top breast cancer features corresponding to the ℓ_1 -PGD-GSVPSVM (top), and ℓ_q -PGD-GSVPSVM methods for $q = 0.1$ (middle) and $q = 1$ (bottom).

are displayed in the last column of Figure 6 for the different methods. We see from Figure 6 that the selected genes can separate normal and cancer classes into distinct blobs in low-dimensional subspaces.

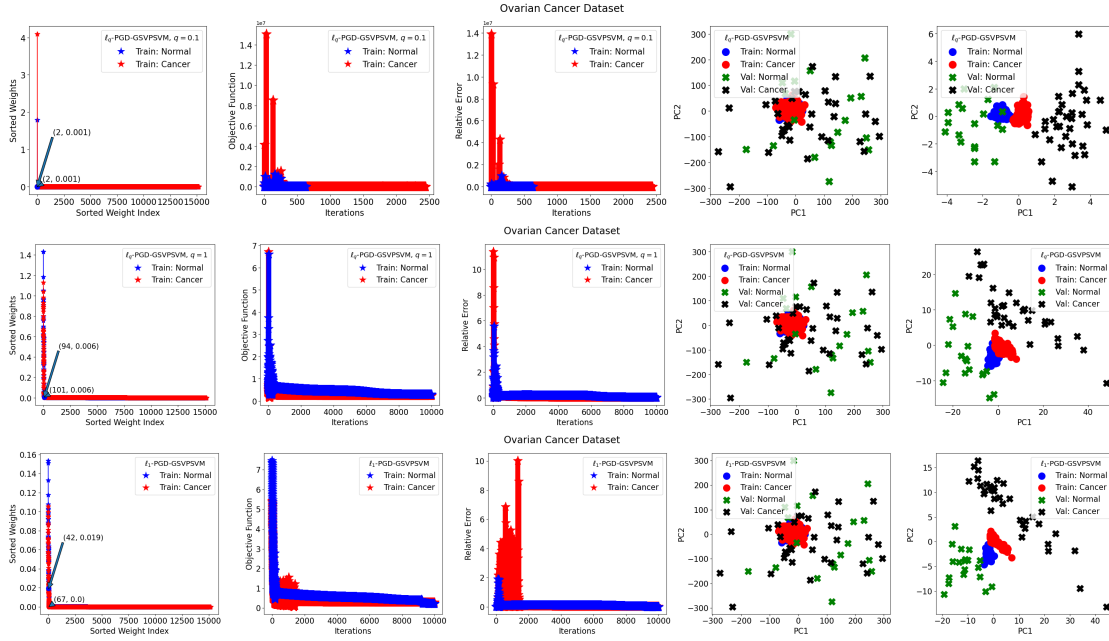


Figure 6: The solutions of the $\ell_{0.1}$ -PGD-GSVPSVM, ℓ_q -PGD-GSVPSVM ($q = 1$), and ℓ_1 -PGD-GSVPSVM methods with PCA plots.

Feature Index (Normal)	Top Features (Normal)	Feature Index (Cancer)	Top Features (Cancer)
0	1678	MZ244.95245	1736
1	182	MZ2.8548732	7281
0	8273	MZ5959.5856	1678
1	8274	MZ5961.0266	1679
2	8275	MZ5962.4677	1680
3	2239	MZ436.24386	1677
4	2240	MZ436.63379	1681
5	8272	MZ5958.1448	2191
6	2236	MZ435.07512	1735
7	2237	MZ435.46452	1682
8	2238	MZ435.85411	1683
9	6381	MZ3545.177	1736
0	8274	MZ5961.0266	2527
1	8273	MZ5959.5856	1678
2	8275	MZ5962.4677	1679
3	2239	MZ436.24386	2528
4	2236	MZ435.07512	1680
5	2240	MZ436.63379	2526
6	2237	MZ435.46452	1681
7	6381	MZ3545.177	1677
8	2238	MZ435.85411	1682
9	8272	MZ5958.1448	1683

Figure 7: Top ovarian cancer genes corresponding to the $\ell_{0,1}$ -PGD-GSVPSVM (top), and ℓ_q -PGD-GSVPSVM, $q = 1$ (middle) and ℓ_1 -PGD-GSVPSVM (bottom) methods.

Dataset	Methods	Bal. Acc.	Specificity	Recall	Precision	TN	FP	FN	TP
Ovarian Cancer (Validation)	ℓ_1 -PGD-GSVPSVM	97.06	100	94.12	100	19	0	2	32
	ℓ_q -PGD-GSVPSVM ($q = 1$)	95.59	100	91.18	100	19	0	3	31
	$\ell_{0,1}$ -PGD-GSVPSVM	100	100	100	100	19	0	0	34
Ovarian Cancer (Test)	ℓ_1 -PGD-GSVPSVM	96.67	100	93.33	100	9	0	1	14
	ℓ_q -PGD-GSVPSVM ($q = 1$)	93.33	100	86.67	100	9	0	2	13
	$\ell_{0,1}$ -PGD-GSVPSVM	100	100	100	100	9	0	0	15

Table 5: Classification reports for the ovarian cancer dataset.

It is noteworthy that [9] utilized 6 genes to achieve 100% classification accuracy on a test set, whereas Table 5 and Figure 7 shows that the $\ell_{0,1}$ -PGD-GSVPSVM method achieved 100% balanced accuracy with only 4 genes. This demonstrates that the proposed approach can result in fewer genes while achieving superior classification accuracy.

6 Conclusions

We have demonstrated that the ℓ_q -PGD-GSVPSVM methods for $0 < q \leq 1$ are viable feature selection and classification techniques that can achieve perfect to near-perfect classification accuracy. The performance of the methods are illustrated using the breast and ovarian cancer datasets. The sparsity levels in the computed solutions are exploited to select a parsimonious set of informative features. For the ℓ_q -PGD-GSVPSVM method, smaller values of q often result in fewer features

being selected. More often than not, the smaller the q , the sparser the solutions determined by the methods. We recommend $0 < q < 0.4$ if a small set of features is desired.

References

- [1] O. Alter, Orly, P. O. Brown, and D. Botstein, Generalized singular value decomposition for comparative analysis of genome-scale expression data sets of two different organisms, *Proceedings of the National Academy of Sciences* 100 (2003), pp. 3351-3356.
- [2] A. Beck, and M. Teboulle, A fast iterative shrinkage-thresholding algorithm for linear inverse problems. *SIAM journal on imaging sciences*, 2 (2009), pp. 183-202.
- [3] J. A. Berger, S. Hautaniemi, S. K. Mitra and J. Astola, Jointly analyzing gene expression and copy number data in breast cancer using data reduction models, in *IEEE/ACM Transactions on Computational Biology and Bioinformatics*, 3 (2006), pp. 2-16. doi: 10.1109/TCBB.2006.10
- [4] M. P. Brown, W. N. Grundy, D. Lin, N. Cristianini, C. W. Sugnet, T. S. Furey, M. Ares Jr, and D. Haussler, Knowledge-based analysis of microarray gene expression data by using support vector machines. *Proceedings of the National Academy of Sciences*, 97 (2000), pp.262-267.
- [5] E. J. Candes, M. B. Wakin, and S. P. Boyd, Enhancing sparsity by reweighted ℓ_1 minimization, *Journal of Fourier Analysis and Applications*, 14 (2008), pp. 877-905.
- [6] Y. Chen, and Z. Yang, Generalized eigenvalue proximal support vector machine for functional data classification, *Symmetry*, 13 (2021), 833. <https://doi.org/10.3390/sym13050833>
- [7] M. T. Chu, R. E. Funderlic, and G. H. Golub, On a variational formulation of the generalized singular value decomposition, *SIAM Journal on Matrix Analysis and Applications* 18 (1997), pp. 1082-1092.
- [8] C. Cortes and V. Vapnik, Support-vector networks, *Machine Learning*, 20 (1995), pp. 273-297.
- [9] T. Elemam, and M. Elshrkawey, A highly discriminative hybrid feature selection algorithm for cancer diagnosis. *The Scientific World Journal*, 1 (2022), pp. 1056490.
- [10] T. S. Furey, N. Cristianini, N. Duffy, D. W. Bednarski, M. Schummer, and D. Haussler, Support vector machine classification and validation of cancer tissue samples using microarray expression data, *Bioinformatics*, 16 (2000), pp. 906-914.
- [11] G. H. Golub, and C. F. Van Loan, (1996) *Matrix Computation*, Johns Hopkins Univ. Press, Baltimore, 4th Ed.
- [12] M. R. Guarracino, M. Sangiovanni, G. Severino, G. Toraldo, and M. Viola, On the regularization of generalized eigenvalues classifiers, in *Proc. AIP Conf.*, 2016, vol. 1776. no. 1, p. 040005.
- [13] M. R. Guarracino, C. Cifarelli, O. Seref, and P. M. Pardalos, A classification method based on generalized eigenvalue problems. *Optim Methods Softw*, 22 (2007), pp. 73-81.
- [14] M. R. Guarracino, Mario Rosario, A. Irpino, and R. Verde, Multiclass generalized eigenvalue proximal support vector machines, In *2010 International Conference on Complex, Intelligent and Software Intensive Systems*, (2010) pp. 25-32. IEEE.
- [15] I. Guyon, J. Weston, S. Barnhill, and V. Vapnik, Gene selection for cancer classification using support vector machines. *Machine Learning*, 46 (2002), pp. 389-422.

- [16] T. Hastie, R. Tibshirani, M. B. Eisen, A. Alizadeh, R. Levy, L. Staudt, W. C. Chan, D. Botstein, and P. Brown, 'Gene shaving' as a method for identifying distinct sets of genes with similar expression patterns, *Genome Biology*, 1 (2000), pp. 1-21.
- [17] I. T. Jolliffe, *Principal Component Analysis*, Springer, (1986), pp. 129–155.
- [18] C. N. Li, Y. H. Shao, and N. Y. Deng, Robust ℓ_1 -norm non-parallel proximal support vector machine, *Optimization* 65 (2016), pp. 169–183.
- [19] O. L. Mangasarian, and E. W. Wild, Multisurface proximal support vector machine classification via generalized eigenvalues, *IEEE Trans Pattern Anal Mach Intell* 28 (2006), pp. 69-74.
- [20] M. H. Memon, P. L. Jian, A. U. Haq, M. H. Memon, and W. Zhou, Breast cancer detection in the IOT health environment using modified recursive feature selection. *Wireless Communications and Mobile Computing* 2019, 1 (2019), pp. 5176705.
- [21] S. O'Hara, K. Wang, R. A. Slayden, A. R. Schenkel, G. Huber, C. S. O'Hern, M. D. Shattuck, and M. Kirby, Iterative feature removal yields highly discriminative pathways, *BMC Genomics*, 14 (2013), pp. 1-15.
- [22] L. Omberg, G. H. Golub, and O. Alter, A tensor higher-order singular value decomposition for integrative analysis of DNA microarray data from different studies, *Proceedings of the National Academy of Sciences*, 104 (2007), pp. 18371-18376.
- [23] N. Parikh, and S. Boyd, Proximal algorithms. *Foundations and Trends in Optimization*, 1 (2014), pp. 127-239.
- [24] B. N. Parlett, *The symmetric eigenvalue problem*, SIAM, Philadelphia, PA, (1998), pp. 357.
- [25] V. Pappu, O. P. Panagopoulos, P. Xanthopoulos, and P. M. Pardalos, Sparse proximal support vector machines for feature selection in high dimensional datasets, *Expert Systems with Applications*, 42 (2015), pp. 9183-9191.
- [26] S. P. Ponnappalli, M. A. Saunders, C. F. Van Loan, and O. A. Alter, higher-order generalized singular value decomposition for comparison of global mRNA expression from multiple organisms, *PloS*, 6 (2011), e28072.
- [27] P. W. Ren, C. N. Li, and Y. H. Shao, Capped-Norm Proximal Support Vector Machine. *Mathematical Problems in Engineering* 2022 (2022).
- [28] Y. H. Shao, N. Y. Deng, W. J. Chen, and Z. Wang, Improved Generalized Eigenvalue Proximal Support Vector Machine, in *IEEE Signal Processing Letters*, 20 (2013), pp. 213-216, doi: 10.1109/LSP.2012.2216874.
- [29] J. Song, P. Babu, and D. P. Palomar, Sparse generalized eigenvalue problem via smooth optimization, *IEEE Transactions on Signal Processing*, 63 (2015), pp. 1627-1642.
- [30] X. Q. Sun, Y. J. Chen, Y. H. Shao, C. N. Li, and C. H. Wang, Robust nonparallel proximal support vector machine with ℓ_p -norm regularization, in *IEEE Access*, 6 (2018), pp. 20334-20347, doi: 10.1109/access.2018.2822546.
- [31] R. Tibshirani, Regression shrinkage and selection via the lasso, *Journal of the Royal Statistical Society: Series B (Methodological)*, 58 (1996), pp. 267-288.
- [32] M. Viola, M. Sangiovanni, G. Toraldo, and M. R. Guarracino, A generalized eigenvalues classifier with embedded feature selection. *Optim Lett*, 11 (2017), pp. 299-311. <https://doi.org/10.1007/s11590-015-0955-7>
- [33] H. Yan, Q. Ye, T. Zhang, D. J. Yu, and Y. Xu, ℓ_1 -norm GEVPSVM classifier based on an effective iterative algorithm for classification, *Neural Process. Lett.*, (2017), pp. 1–26.
- [34] S. Zhou, X. Xiu, Y. Wang, and D. Peng, Revisiting ℓ_q ($0 \leq q < 1$) Norm Regularized Optimization, (2023). <https://arxiv.org/pdf/2306.14394.pdf>